

# Smart participation of PHEVs in controlling voltage and frequency of island microgrids

Bahram Pournazarian<sup>a</sup>, Peyman Karimyan<sup>b,\*</sup>, G.B. Gharehpetian<sup>b</sup>, Mehrdad Abedi<sup>b</sup>,  
Edris Pouresmaeil<sup>a</sup>

<sup>a</sup> Department of Electrical Engineering and Automation, Aalto University, Espoo, Finland

<sup>b</sup> Department of Electrical Engineering, Amirkabir University of Technology, Tehran, Iran

## ARTICLE INFO

### Keywords:

Microgrid (MG)  
Plug in hybrid electric vehicles (PHEVs)  
Voltage control  
Frequency control  
Intelligent droop control  
Smart charging strategy

## ABSTRACT

The microgrids (MGs) are composed of several Distributed Generation (DG) units, storages and loads at the demand side which can work in both islanded and connected to the main grid; in islanded mode, the MGs voltage and frequency must be controlled by individual DG units. As the Plug-in Hybrid Electric Vehicles (PHEVs) in MGs can have both roles of loads and storages, participation of these ever growing elements in the MGs voltage and frequency control problem is investigated in this study. At first, an intelligent droop control for MGs voltage and frequency control is proposed to be implemented on inverter-interfaced DGs except PHEVs. The proposed droop control is independent from the MG lines parameters and can control the voltage and frequency of MG seamlessly. Afterwards, a novel strategy for participating the PHEVs in controlling the voltage and frequency of MGs is proposed. This strategy is implemented on the PHEVs parking lots in the Vehicle-to-grid (V2G) mode. This strategy has a prominent capability to keep the stability of MG even in severe scenarios compared to the other previous strategy. Moreover, the proposed strategy lowers the voltage drops and keeps the frequency constant. In the simulation studies, both proposed (named smart) and previous (named non-smart) charging strategies are implemented and compared. The simulation results show the effectiveness of the proposed strategy in order to keep the stability of MG even in severe scenarios, maintain the frequency and voltage better than another recent strategy.

## 1. Introduction

The microgrid (MG) is defined as a low-voltage network consisting various DGs, energy storage systems (ESSs) and loads which could be either islanded or connected to the main grid [1]. In the grid connected mode, the micro-sources (MS) operate in the mode of control of active and reactive powers (called PQ), but in the islanded mode of operation, the MSs are responsible to maintain the voltage and frequency of the MG, namely, operate as voltage source inverter (VSI) [2]. In an islanded (isolated) MG including several MSs; like a power system consisting of several generators, the droop strategy has been suggested in order to control the voltage and frequency of MGs [3]. The droop control has been under research for several years. In [4], a new intelligent droop control has been suggested which can be applied to all kinds of MGs (inductive, resistive or their combination). The another droop control in [5] proposed new droop control equations to consider both resistance and reactance of lines in MG. The angle droop control for decoupling

the active and reactive power controls was proposed in [6] to have less steady state frequency deviation in the active power control in comparison with the conventional droop control. The robust transient droop function proposed in [7] tends to attenuate the low-frequency oscillations originated from conventional droop control method by evaluating the specific ranges for transient droop gains; the Kharitonov's stability theorem was used to do this analysis.

Reviewing all the recent researches reveals that the Artificial Intelligent (AI) methods are going to play a prominent role to address the problems in MG, e.g. the small signal instability is resolved in [8] and the overall application of AI methods for MG control are reviewed in [9,10]. Novel meta-heuristic optimization strategies proposed to implement on PHEVs was reviewed in [11] which recommends the future prospects in this field of research. Some bio-inspired computational intelligence (CI)-based optimizations for Plug in Electric Vehicles charging are also introduced and reviewed in [12].

On the other hand, Because of the intermittent nature of renewable

\* Corresponding author at: Amirkabir University of Technology (Tehran Polytechnic), No. 424, Hafez Ave., Tehran 15914, Iran.

E-mail addresses: [bahram.pournazarian@aalto.fi](mailto:bahram.pournazarian@aalto.fi) (B. Pournazarian), [peyman.karimyan@aut.ac.ir](mailto:peyman.karimyan@aut.ac.ir), [peyman.sena@gmail.com](mailto:peyman.sena@gmail.com) (P. Karimyan), [grptian@aut.ac.ir](mailto:grptian@aut.ac.ir) (G.B. Gharehpetian), [Abedi@aut.ac.ir](mailto:Abedi@aut.ac.ir) (M. Abedi), [edris.pouresmaeil@aalto.fi](mailto:edris.pouresmaeil@aalto.fi) (E. Pouresmaeil).

<https://doi.org/10.1016/j.ijepes.2019.03.036>

Received 20 October 2018; Received in revised form 27 February 2019; Accepted 18 March 2019

0142-0615/ © 2019 Published by Elsevier Ltd.

energy sources (RES), output powers of them are fluctuating. The ESSs can play a complementary role behind the RESs, in order to deliver a constant power to the MG [13]. batteries as a well-known kind of ESSs have been under attention as a candidate to use in the MG either individually or with intermittent DGs. In [14] a new frequency controller combining conventional droop control and an inertia element has been proposed to control the Battery energy storage system (BESS) during the primary frequency control of isolated MG. The secondary control framework proposed in [15] tends to use conventional droop control and an state of charge (SOC) estimation method, to design a new storage controller which restores the voltage and frequency of the stand-alone MG, this control strategy requires a communication link between neighbour ESSs. The benefits of utilizing a BESS in an hybrid diesel-wind system has been mentioned as a main contribution of [16] which presents several simulation cases. A frequency-based energy management method for multiple energy storage units has been proposed in [17] which uses a modified droop control and makes it possible to regulate the current and voltage of individual batteries, avoiding from under-discharge and over-discharge of batteries. The dynamic energy balancing method in [18] tends to improve the frequency regulation in a MG through a multi-agent control system which monitors the output power of different storage systems based on a droop characteristic.

Plug-in Hybrid Electric Vehicles (PHEVs) are essentially BESS which are going to be more and more used in future MGs. Several researches have been conducted on electric vehicles charging in MG. The PHEVs charging imposes a load to the MG, but bidirectional chargers can prepare the possibility of injecting the energy from vehicle to the grid [19]. The idea of using electric vehicles (EVs) batteries in load frequency control (LFC) problem has been introduced in [20] proposing a novel robust strategy using a combination of Fuzzy Logic Sets and the Modified Harmony Search Algorithm to tune the PI controllers. Using linear quadratic theory, the LFC problem has been solved in an island MG including several micro sources to reduce the frequency deviation [21]. In [22], the optimal number of PHEV's parking lots in the MG has been determined by a new genetic algorithm (GA) based methodology, which aims at minimization of the total cost. In [23], the charging and discharging of PHEVs and the SOC control has been presented using an improved model predictive control. In [24], the EVs have participated in the primary frequency control of an island MG, only in charging mode. The proposed MG had a large penetration of intermittent RESs. In other words, the proposed strategy has determined the charging capacity of battery, based on the MG frequency. In [25] different types of charging of PHEVs and EVs have been reviewed, any charging method is suitable for special application and environment, also, the optimization methods for charging regimes have been reviewed. The charging level-1 requires a regular single-phase outlet as a normal home charging. The charging level-2 rates up to 19.2 kW and 240 V single phase charging power and charging level-3 which can be connected to a three-phase urban station at 480 V or higher voltage. Finally, in [26], the participation strategy of EVs has been developed to consider both charging and discharging mode of operation. The proposed droop control consists of an additional loop (called inertial emulation) for primary frequency control of isolated grids.

Considering all aforementioned methods, this study tends to propose an intelligent droop control method; which is an advanced form of a previous strategy which is independent from the lines parameters. This droop control tends to be implemented on all inverter-interfaced DGs in MG except the PHEVs parking lot. Afterwards, a novel charging strategy for the PHEVs parking lot is proposed which could do the best to keep the stability of the island MG and accomplishes its primary voltage and frequency control. The proposed strategy doesn't require any communication link. It is based on the idea that in a real MG both voltage and frequency are mutually dependent because of the parameters of lines which are resistive-inductive; so, the injection of active power could enhance the voltage and frequency of island MG. The proposed charging framework monitors both voltage and frequency of

the MG to make an active power command for PHEVs interface inverter. Considering the three-phase interconnecting inverter and the rate of charging power, this charging method can be adopted in level-3 charging structures directly. Eventually, a 14-bus isolated MG consists of diesel generator, PV panels, Fuel Cells and PHEVs, is implemented in the Matlab/Simulink environment. Two strategies are implemented on PHEVs parking lot, one previous strategy (named non-smart strategy) and the proposed novel strategy (named smart strategy). It is shown that the primary voltage and frequency control is done effectively by the smart strategy better than the other previous strategy. The critical role of PHEVs is prominent in the both voltage and frequency controls. The proposed smart strategy insures that the PHEVs charging and discharging supports the stability of MG better than the other recent strategy.

The major contributions of this study are as follows:

- Presenting an intelligent droop control for island MGs which is independent from the lines parameters.
- Proposing a novel strategy for PHEVs to participate in the primary voltage and frequency control of island MGs so as to keep the stability of island MG.

The rest of this paper is organized as follows; Section 2 introduces island MGs voltage and frequency control framework. Section 3 is devoted to PHEVs modelling and their participation strategy. Simulation studies consisting two scenarios, are described in Section 4. Afterwards, the conclusion is drawn from this study in Section 5. Eventually, the future research horizons and prospects are proposed in Section 6.

## 2. Island MGs voltage and frequency control

The practical MGs consist of both renewable and non-renewable resources, They should effectively be controlled so as to deliver acceptable frequency and voltage to the loads. Like traditional power systems with several generators, a droop control strategy can be implemented in order to control the voltage and frequency of MG and keep the stability of it [27]. Following the droop control strategies for inverter-interfaced DGs are introduced and proposed. Definitely the proposed intelligent droop control didn't aim at the other micro-sources like diesel-generators or PHEVs.

### 2.1. Conventional droop control for voltage and frequency control of island MG

Consider a simple MG consisting a load, a generating unit and a line between them as shown in Fig. 1. The active and reactive powers flowing in the line, are as follows [4]:

$$P = \frac{V_S}{(R^2 + X^2)} [R(V_S - V_L \cos \delta) + X V_L \sin \delta] \quad (1)$$

$$Q = \frac{V_S}{(R^2 + X^2)} [-R V_L \sin \delta + X (V_S - V_L \cos \delta)] \quad (2)$$

Based on the assumption that the lines are inductive, we have [28]:

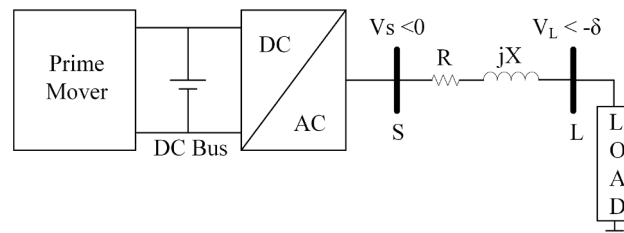


Fig. 1. Microgrid supplying load via three phase line.

$$\delta = \frac{XP}{(V_S V_L)} \quad (3)$$

$$V_S - V_L = \frac{XQ}{(V_S)} \quad (4)$$

Considering (3) and (4), it is obvious that in order to adjust the frequency ( $\delta$ ), the active power must be controlled. Which is called P/f control. A similar explanation could be followed for controlling the voltage. Also the reactive power which controls the voltage of the VSC connected to the MG, which is called Q/V control, similarly [28].

The traditional droop controls for controlling the voltage and frequency of the MG are [29]:

$$f - f_0 = -k_p(P - P_0) \quad (5)$$

$$V_S - V_{s0} = -k_q(Q - Q_0) \quad (6)$$

Defining  $f_0$  and  $V_{s0}$  as the nominal values of frequency and voltage of the MG, the droop coefficients ( $k_p$  and  $k_q$ ) determine the basic operation of inverter-based DG against changes in voltages and frequency. Once the frequency falls down, the inverter increases the output active power, just like a synchronous generator. A similar argument tends to be used about the changes in voltage and its consequent deviation in the reactive power generation.

## 2.2. The overall droop controllers (ODC) for voltage and frequency control of island MG

Considering this point that in the MG one could not rely on this assumption that transmission lines are pure inductive, the basic idea has been introduced in [5] which are linearization of (1) and (2) around an operation point as follows:

$$\Delta P|_{(\delta_0, V_{s0})} = \frac{\partial P}{\partial \Delta} \cdot \Delta \delta + \frac{\partial P}{\partial V_S} \cdot \Delta V_S \quad (7)$$

$$\Delta Q|_{(\delta_0, V_{s0})} = \frac{\partial Q}{\partial \Delta} \cdot \Delta \delta + \frac{\partial Q}{\partial V_S} \cdot \Delta V_S \quad (8)$$

Using (7) and (8), The following equations can be written as[5]:

$$\Delta f = \frac{1}{2\pi} \cdot [X \cdot \Delta P - R \cdot \Delta Q] \quad (9)$$

$$\Delta V_S = R \cdot \Delta P + X \cdot \Delta Q \quad (10)$$

In case of MG seen in Fig. 1, both  $R$  and  $X$  are known and these droop control equations could be straightforward and applicable. So, the following infrastructure is proposed for a VSI in MG.

The proposed control structure in Fig. 2 has several subsystems which are defined as follows.

### 2.2.1. ODC controllers

The ODC-f controller implements the Eq. (9), it receives the active and reactive power values in p.u and generates the  $\Delta f$  command. The ODC-V controller implements the Eq. (10), it receives the active and reactive power values in p.u and generates the  $\Delta V$  command.

### 2.2.2. Power controller

This unit calculates the instantaneous active and reactive powers using d-q frame components of voltage and current[29].

$$\begin{cases} p = (V_d I_d + V_q I_q) \\ q = (V_d I_q - V_q I_d) \end{cases} \quad (11)$$

$$\begin{cases} P = \left( \frac{\omega_c}{s + \omega_c} \cdot p \right) \\ Q = \left( \frac{\omega_c}{s + \omega_c} \cdot q \right) \end{cases} \quad (12)$$

In (12),  $\omega_c$  is cut-off frequency of low-pass filter and it is assigned based on our problem. All in all, this unit delivers the active and reactive

powers to the intelligent droop controllers unit. In order to remove unwanted harmonics, a low-pass filter is applied after power controllers.

### 2.2.3. Voltage controller

The voltage control block including feed-forward and feedback loops, generates the current commands in d-q frame. The operation of this unit could be summarized in the following equations:

$$\begin{cases} i_{ld}^* = F i_{od} - \omega_c F v_{oq} + (K_{pv} + \frac{K_{iv}}{s})(v_{od}^* - v_{od}) \\ i_{lq}^* = F i_{oq} + \omega_c F v_{od} + (K_{pv} + \frac{K_{iv}}{s})(v_{oq}^* - v_{oq}) \end{cases} \quad (13)$$

In (13),  $\omega_c$  is the angular velocity of the system (or the velocity of the synchronous rotational frame). The parameter  $F$  is the feed-forward coefficient assigned to have low external impedance and enhance the operation of the system.  $K_{pv}$  and  $K_{iv}$  are controller's coefficients which can be assigned using classic zero-pole, bode diagram or an optimization method [29].

### 2.2.4. Current controller

The current controller generates the voltage commands for PWM switching unit. The operation of this unit is stated by (14).

$$\begin{cases} v_{ld}^* = -\omega_c L_f i_{lq} + (K_{pc} + \frac{K_{ic}}{s})(i_{ld}^* - i_{ld}) \\ v_{lq}^* = \omega_c L_f i_{ld} + (K_{pc} + \frac{K_{ic}}{s})(i_{lq}^* - i_{lq}) \end{cases} \quad (14)$$

It is proposed that the bandwidth of the current controller should be about 1.6 kHz [29].

### 2.2.5. Output LC filter

It is proposed that in order to reduce the voltage ripple, as a rule of thumb, the resonance frequency of LC filter should be 10 times smaller than the switching frequency[5].

## 2.3. Intelligent droop controls for voltage and frequency control of island MG

When coming to analyze a complicated MG including several MSs, it seems impractical to use previously-defined ODC controllers, because the values of equivalent  $R$  and  $X$  between any MS and the load are not clear. In [4] it is proposed to use Adaptive neuro fuzzy inference system training to train ODC blocks in the simple MG (Fig. 1) and then integrate these trained controllers into more complex MGs. Using this method, the ODC controllers become general blocks independent of  $R$  and  $X$ . In this regards, based on the proposed method in [4], an VSI is installed in a simple MG as seen in Fig. 1, two arbitrary values for  $R$  and  $X$  are selected. Then the values of active and reactive powers of load are changed according to a scenario in Table 1. The necessary data about the inverter parameters are enclosed in the appendix. Three sets of  $R$  and  $X$  are considered, i.e.  $R = 0.1$ ,  $X = 1$ ,  $R = 1$ ,  $X = 0.1$  and  $R = 1$ ,  $X = 1$ . for any of these three sets, the VSI in the simple MG of Fig. 1 is installed and the load changing scenarios of Table 1 are implemented from  $t = 1$  s to  $t = 3$  s. The data of  $P$ ,  $Q$ ,  $\Delta f$  and  $\Delta V$  are saved in a separate table. then the another sets of  $R$  and  $X$  is used and this data saving is repeated. Finally, using the gathered data of  $P$ ,  $Q$ ,  $\Delta f$  and  $\Delta V$  two separate (two-input one-output) ANFIS controllers are trained. The training method is well-described in [4], so it didn't seem necessary to be repeated here. The ANFIS trained controllers will be used in the MG as it is seen in Fig. 3.

## 3. PHEVS modelling and participation strategy

PHEVs play both the role of loads and storage systems. The first step is to introduce their model in the MG voltage and frequency control problem. The next step is to define an advanced strategy to effectively



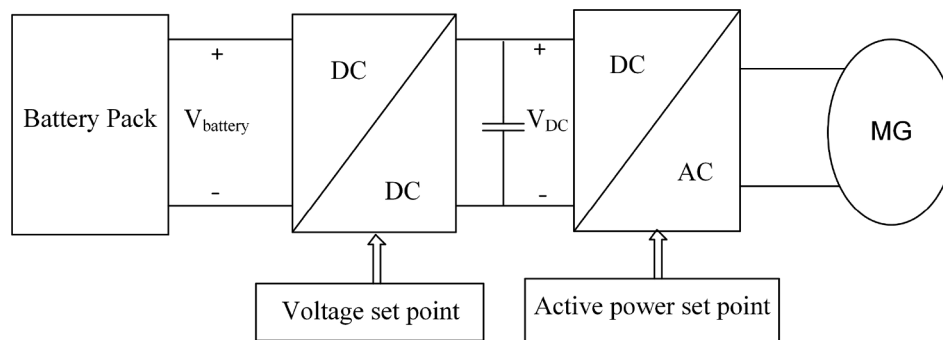


Fig. 4. Implemented model for bidirectional charging of PHEVs in MG[31].

is portrayed in Fig. 4 which consists of a battery pack, a DC-DC converter and an interface inverter connected in series as introduced in [31]. It should be noted that, In the scope of this study, PHEVs are considered to be charged in a parking lot in the islanded MG, to the best of the authors knowledge, all available chargers are connected to the grid via wire and plug, consequently, during the charging or injecting to the grid the individual vehicles demand are negligible because they are parked without movement, so the battery of the vehicle and the interface converters are the main parts playing the role in connection to the MG. Another point is that the state of charge (SOC) of the batteries doesn't change instantly, so in a short-time dynamic study like ours; which has simulations during 12 s time interval, it can be assumed that the SOC of PHEVs vehicles are constant. So the difference in the vehicles batteries SOC's and batteries types cannot affect the scope of this study and its results.

Following assumptions are considered in the proposed PHEVs model:

- The PHEVs SOC's assumed to be constant, since the study duration is short.
- The PHEVs are either charged or inject power to the MG in one parking lot, they are assumed as an aggregated unit in this dynamic study.
- The individual PHEVs demands during the short time of charging in this study are negligible.

### 3.2. Novel Participation strategy for PHEVs

In an isolated power system according to European Norm EN50160, the standard permitted frequency deviation is  $\pm 1$  Hz. On the other hand, according to IEEE Std 1547.2-2008, the permitted voltage deviation is  $\pm 5\%$  [32].

It is proposed that PHEVs parking lot including several PHEVs could be controlled in the active power control mode in order to support the other MSs which are responsible for voltage and frequency control in an island MG. In addition to all traditional methods of voltage control such as tap-changing of transformers or capacitor-switching, PHEVs should facilitate the voltage control in MG in emergency cases by injecting the active power. Even though this is not an economical procedure, but it is worth stabilizing the MG in emergency cases.

The method introduced in [26] has proposed to generate an active power command considering the frequency deviation and its derivative to participate the Electric Vehicles (EVs) into the frequency control of power systems, this method could be seen in Fig. 5 as the previous participation strategy(non-smart charging). Considering the previous strategy, it is proposed that in case of island MGs, the voltage control loop could be placed in the control strategy of PHEVs parking lot so as to mimic the mutual dependency of voltage and frequency in a real MG and better controlling the voltage and frequency of island MGs. The novel proposed strategy is demonstrated in Fig. 6.

The proposed participation strategy of PHEVs in an island MG is

written as follows:

$$\Delta P_{fc} + \Delta P_{vc} + \Delta P_{contract} = P_{PHEV} \quad (15)$$

$$\begin{cases} \Delta P_{fc} = k_p \Delta f + k_{in} \cdot \frac{d}{dt} \Delta f \\ \Delta P_{vc} = (K_p + \frac{K_i}{s}) \cdot \Delta V \end{cases} \quad (16)$$

where

- $\Delta P_{fc}$  is PHEV's active power devoted to frequency control
- $\Delta P_{vc}$  is the PHEV's active power devoted to voltage control
- $P_{PHEV}$  is the total active power of PHEVs is consumed by MG
- $P_{contract}$  is the nominal power of PHEVs according to a contract between PHEV's parking lot and the MG; it is worthy to mention that in normal mode of operation this value is equal to total active power of PHEVs.
- $k_p, k_{in}, K_p, K_i$  are coefficients of voltage and frequency control which must be assigned according to the circumstances.

One significant point is that PHEVs must not respond to any trivial voltage or frequency deviation; they will exchange their contracted powers in these situations in order to charge their batteries. So, practical dead-bands are considered in the proposed participation strategy. These dead-bands cause the PHEVs to get rid of redundant charging and discharging. Also, the excessive cost is not spent by MG operator or owner. As a matter of fact, this is a beneficial and necessary compromise between an aggregator and PHEV's owner.

The reference active power is assigned in several ways:

- In case of having PHEVs which are responsible to the frequency and voltage control strategy, the active power set-point is determined by parking lot (or aggregator); these PHEVs are participants of MG's control program.
- Considering the rest of vehicles, which behave like a kind of loads connected to the MG, the active power set point is determined according to the contract (the nominal power is consumed).

To show all possible scenarios for any PHEV in the MG, the following schematic diagram is provided. As the Fig. 7 demonstrates, the smart charging strategy tends to get the voltage and frequency feed-backs from the connection point and decide about the statues and the amount of charging or injecting active power to the MG. In order to more clarify and differentiate between the smart charging and the other charging strategy (named non-smart), Table 2 lists the characteristics of both strategies.

To sum up the main contributions of the current study, the advantages and disadvantages of the proposed smart charging method are reviewed in Table 3 which can spotlight the research horizons and future works.

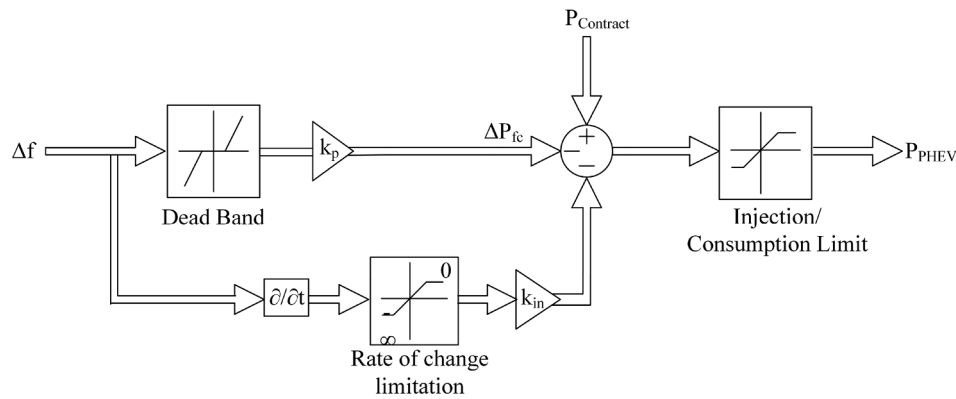


Fig. 5. Previous (non-smart charging) control strategy of PHEVs parking lot connected to an island MG [26].

#### 4. Results and discussion

Two simulation scenarios are considered and implemented. In the first scenario, the PHEVs participate in the frequency control of MG according to the previous strategy shown in Fig. 5, and in the second one, the PHEVs cooperate in the voltage and frequency control of MG utilizing the novel proposed strategy named as smart-charging strategy demonstrated in Fig. 6.

##### 4.1. MG under study and its DGs

A 14-bus MG introduced in [4] is modified and then simulated as depicted in Fig. 8. All loads are 4.5 times bigger than the original case. The data of this MG are summarized in Tables III and IV in the Appendix. They list the loads and the lines impedances of this 14-bus test MG, respectively.

A 100 kW diesel generator equipped with a fixed-speed IEEE type 1 governor is selected from MATLAB/ Simulink library and installed in bus 14.

A PV system including 88 parallel strings and 7 series strings are selected from MATLAB/ Simulink library (SunPower SPR-415E-WHT-D) and embedded in bus 11. The PV system is supported by a storage battery located on its dc bus, namely 200 V, 200 Ah Li-Ion battery charged by PV and delivering a fixed dc voltage to the inverter.

The third DG consists of two proton exchange membrane fuel-cell (PEMFC)-50 kW- 625 Vdc units which are connected to the MG via a

midpoint dc-dc buck converter and a midpoint inverter controlled by the suggested droop control. The parameters of the mentioned buck converter are listed in Table 4 and the inverter specifications are listed in Table 8 in the Appendix. more detail about converter parameters can be found in [33]. In continues mode of operation of a buck converter we should have the parameters to fulfill this inequality to minimize the ripple:

$$f_s \gg \sqrt{LC}$$

where  $f_s$ , L and C are switching frequency, inductor and capacitor values, respectively.

One parking lot is modeled as two sets of batteries connected to a midpoint full-bridge inverter (current mode controlled). The specifications of the designed interface inverter and corresponding inter-connection impedance are given in Table 5. For all other DGs (PV and PEMFC), the intelligent droop control is implemented. The specification of these two inverters are identical, summarized in Table 8 of the Appendix.

##### 4.2. Initial assumptions

Following assumptions are considered in the simulation studies:

- DG units are PV, PEMFC and diesel generator connected to the buses 7, 11, 14, respectively.

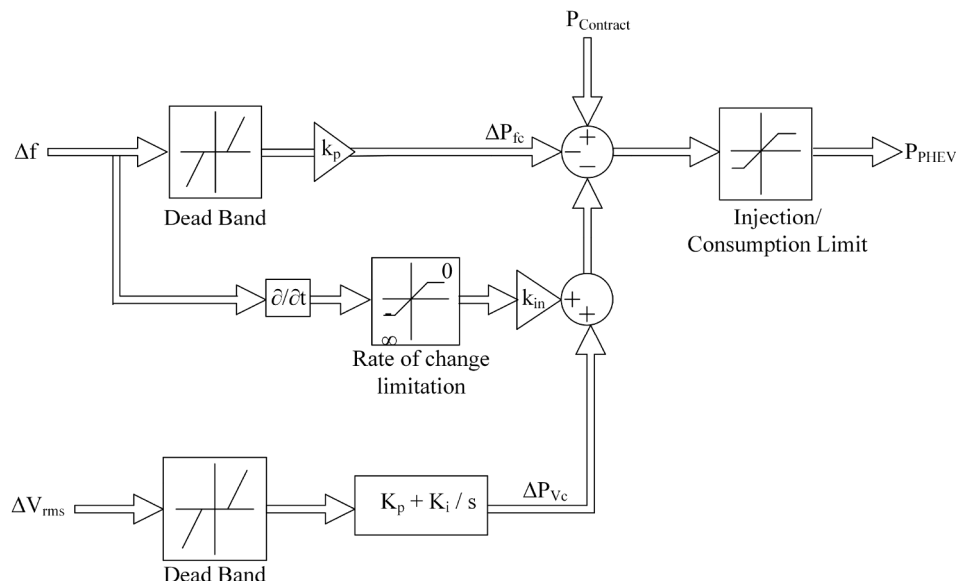


Fig. 6. Proposed control strategy (smart charging) of PHEVs parking lot connected to an island MG.

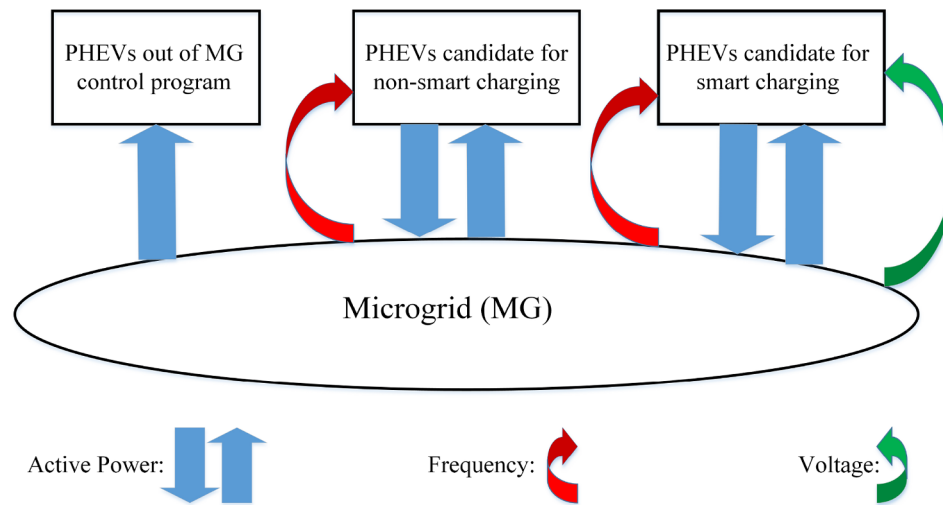


Fig. 7. Schematic diagram of different strategies for a PHEV in MG.

Table 2

The main characteristics of the proposed (smart-charging) and previous (non-smart charging) strategies for PHEVs charging.

Characteristic	Smart-charging	Non-smart charging
Frequency control	✓	✓
Voltage control	✓	×
Bidirectional power exchange	✓	✓

- The solar radiation change is considered, and PV unit is supported by a storage device in order to cover the power fluctuations.
- The interface VSIs between DG units and the MG have practical limits with respect to the current flowing through the IGBTs, and this limit is enforced to the  $d$ -component of the reference current.
- The MG is considered to be island, so the voltage and frequency of the MG must be controlled by DG units.
- The PHEVs are aggregately considered as a parking lot in the bus 13 of the MG. The bidirectional arrow in Fig. 8 implies that PHEVs have a dual role (either absorb or inject active power).
- As some of the PHEVs are connected to the MG while their batteries are fully charged, it is proposed that the maximum injectable power of the parking is larger than its charging power.
- In [26] is proposed that, since the simulation time is short, the state of charge of batteries remain relatively unchanged, so the DC-DC converter in the PHEVs model can be neglected in simulation studies and the individual bridge inverter is considered connected to the battery sets.

#### 4.3. Scenarios: charging using the previous strategy (non-smart charging) and charging using the novel strategy (smart charging)

In non-smart charging (scenario 1), the PHEVs parking lot installed in bus 13 starts its charging based on the previous strategy introduced in Fig. 5 at  $t = 2s$ . Then the load of bus 9 at  $t = 3s$  is increased by 70 kW. Three DG units (diesel, PV and fuel cell) are responsible for controlling the voltage and frequency of MG using the proposed

intelligent droop control. Afterwards, at  $t = 5s$  the sun irradiation falls from 200 to 50 W/m<sup>2</sup>. The PV system is equipped with a storage battery to cover these changes. Subsequently, at  $t = 8s$ , PEMFC will shut down instantly, following this event, examining the behavior of diesel generator and PV and PHEVs parking lot will be quite instructive. The interfacing inverter has practical current limit on its  $d$ -axis current. In this scenario, the frequency and its derivative are sensed to produce the power command for PHEVs parking lot.

In smart charging (scenario 2), the PHEVs parking lot is charged using the proposed novel strategy, shown in Fig. 6, to effectively co-operate in controlling the voltage and frequency of the MG. The charging capacity is about 60 kW and the injection capacity is 80 kW according to the circumstances of the MG. The PHEVs parking lot is sensitive to both voltage and frequency of the MG and in critical situations, will cease its charging and will go to the mode of injecting active power. The chain of events in this scenario are exactly the same as the former scenario, just the behavior of PHEVs parking lots are different.

##### 4.3.1. MG frequency

In Figs. 9 and 10, the frequency of the MG is depicted throughout the scenarios 1 and 2, respectively. Reviewing scenario 1 in Fig. 9, beginning at  $t = 1s$  a chain of events are happened. The frequency is nearly 50 Hz before  $t = 2s$ , then the PHEVs parking lot begins its Non-smart charging by drawing around 60 kW active power (as depicted in Fig. 15). This event causes a small deviation (about 0.1 Hz) in the frequency of the MG. Then at  $t = 3s$ , a load change is happened in bus 9, the instantaneous fall of frequency is 0.3 Hz. Both PV and PEMFC act according to the intelligent droop characteristic and the Diesel also has its conventional governor response (slow response because of its inertia). The Diesel generator restores the frequency to its nominal value (50 Hz) by  $t = 3.6s$ . Afterwards, the sun irradiation decreases from 200 to 50 W/m<sup>2</sup> at  $t = 5s$ , but the storage covers this event and the frequency of the MG is constant. By  $t = 8s$ , the MG has been stable and its frequency was 50 Hz. Following the outage of PEMFC at  $t = 8s$ , the other two units (PV and diesel) are not able to compensate this lack of

Table 3

The main pros and cons of the proposed smart-charging strategy for PHEVs charging.

Advantage	Disadvantages
Keeping the MG's stability Supporting the voltage and frequency of MG Applicable to both single-phase and three phase chargers	Fixed location of parking lot in MG Requiring a secondary voltage and frequency control to restore the nominal values Ignoring the differences in PHEVs batteries and SOC of batteries

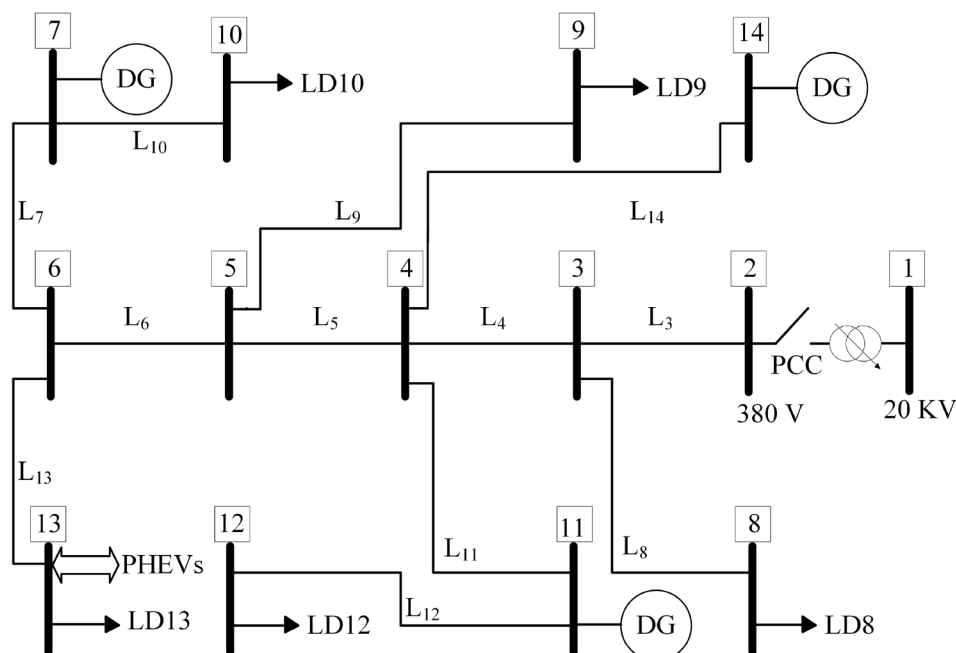


Fig. 8. Simulated 14-bus test MG under study.

**Table 4**  
Specifications of DC-DC buck converter.

Parameter	Value
L	$350 \times 10^{-5} H$
C	$250 \times 10^{-6} F$
$f_s$	5 kHz
$V_{ref}$	500 V
$K_P$	0.01
$K_I$	0.1

**Table 5**  
Specifications of PHEVs interface inverter.

Parameter	Numerical value or transfer function
DC voltage at the inverter's input	500 V
resistance of interface impedance (R)	$0.75 \Omega$
reactance of interface impedance (X)	$0.01 \Omega$
d-axis component in current controller	$375 + (250/s)$
q-axis's component in current controller	$375 + (250/s)$
Feed-forward transfer function ( $G_{ff}(s)$ )	$1/(8 \times 10^{-3}s + 1)$

active power quickly, So the MG enters unstable region and the frequency collapse can be seen. The PHEVs aggravate the situation by drawing active power according to the previous strategy which has no supervision on the voltage of MG.

Fig. 10 shows the frequency of the MG in scenario 2. The PHEVs parking lot starts its charging at  $t = 2s$  causing a small frequency deviation (about 0.05 Hz). Then at  $t = 3s$ , since the load change happens in bus 9, a frequency drop by 0.2 Hz can be seen, but the DGs recover the frequency using the support of PHEVs parking lot which lowers its charging power. Then, the sun irradiation decreases from 200 to 50 W/m<sup>2</sup> at  $t = 5s$ , but the storage supports the PV and the frequency remains unchanged. At  $t = 8s$  PEMFC shuts down and stops injecting power to MG, subsequently, the parking lot injects active power to compensate this severe lack of active power. The fast response of PHEVs parking lot rescues the MG from unstable mode of operation and the

frequency is restored to 50 Hz after a 2s transient.

#### 4.3.2. MG voltages

The voltages of DGs and load bus (i.e., bus 9) are demonstrated in Figs. 11 and 12 for scenarios 1 and 2 respectively. Firstly, Non-smart charging scenario is scrutinized according to Fig. 11. Considering this figure, at  $t = 2s$ , PHEVs parking lot is activated in the mode of charging from MG at bus 13. At this instant, an insignificant voltage drop appears at bus 9. Then, after a 70 kW load switching at bus 9 at  $t = 3s$ , the voltage of PV falls down. This event is related to the upper limit of the inverter current. In reality, by load switching, its major part is going to be supplied by PEMFC and diesel generator, since the PV inverter reached its upper limit during the previous event, it does not answer to this event and subsequently a voltage drop is evident. At  $t = 5s$ , because of a drop in the sun irradiation, the storage battery compensates the lack of active power and it could fix the dc voltage in the input port of the inverter. The outage of PEMFC at  $t = 8s$  causes the MG to become unstable and voltage collapse of all the buses.

To assess the smart charging mode, Fig. 12 is under the spotlight. In this figure, the PHEVs parking lot starts its intelligent charging at  $t = 2s$ , which causes a negligible voltage drop at bus 9. Subsequently at  $t = 3s$ , a load change has happened at bus 9 which causes a voltage drop of 25 V at bus 9, but the voltage at bus 7 is restored to a large degree by lowering the charging power of PHEVs parking lot. The remaining voltage drops must be removed in the secondary voltage control which is out of the scope of this study. The fall in irradiation at  $t = 5s$  does not affect the voltage because of the aforementioned reason. Afterwards, at  $t = 8s$  since the PEMFC shuts down; the PHEVs parking lot changes its mode of operation from charging to injecting active power. As a result, it prevents from instability and the voltages of buses reduce without any collapse occurrence. Even though the voltage drop in bus 9 is more than the standard level (5%), it could be compensated by another alternative method in secondary voltage control.

#### 4.3.3. Powers of DGs

Figs. 13 and 14 demonstrate the DGs powers in scenarios 1 and 2, respectively. In scenario 1, at first, PEMFC generates active power by 95 kW. At  $t = 2s$ , following the starting of PHEVs charging process, the

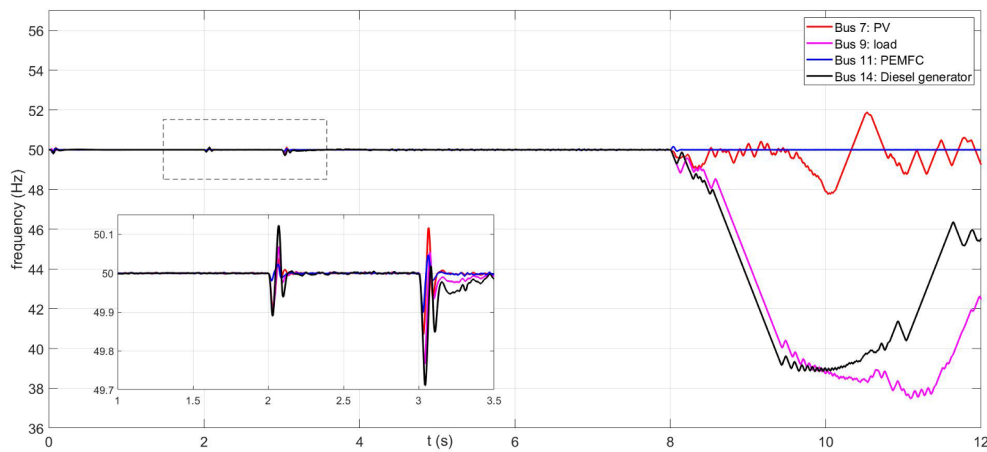


Fig. 9. MG frequency in scenario 1.

PV unit has provided the major part of active power because it is the nearest to the parking lot. The diesel generator and PEMFC participation are negligible. Consequently, following the switching of load at bus 9 at  $t = 3$  s, the major portion of power is served by PEMFC and the diesel generator and the PV response to this event is minor. At  $t = 5$  s, a sudden fall in the sun irradiation happens, but the storage unit covers this change by injecting more current to the dc bus. The active powers of all units are constant which shows the effective role of the storage. Consequently at  $t = 8$  s, because of sudden shut down of PEMFC the powers balance is violated and the MG enters instable mode of operation which is visible as an undamped swing in Fig. 13. The PHEVs, by drawing an amount of active power from the MG according to the previous scenario, worsen the situation and lead the MG towards the instability. When the MG becomes unstable, the charging of them couldn't be done and its disruption is evident in Fig. 15.

Focusing on Fig. 14, the powers of DGs in scenario 2 have been depicted while the PHEVs participate in the intelligent voltage and frequency control methodology. At  $t = 2$  s, following the starting of PHEVs charging process, the major amount of power has been provided by PV unit and the other units haven't reacted to this event prominently. At  $t = 3$  s following a load change event (by 70 kW), about 20 kW has been provided by PEMFC and about 20 kW has been served by diesel generator. Also, the PHEVs parking lot has supported the DGs by lowering its charging power from 60 kW to 20 kW (as seen in Fig. 16). Then at  $t = 5$  s, as the sun irradiation had decreased, the PV power has been constant because of the sESS operation. At  $t = 8$  s when the PEMFC unit has stopped supplying the MG, a large portion of power has been served by PHEVs charging station which has been nearly

80 kW (demonstrated in Fig. 16) and the slow Diesel Generator has generated about 50 kW to cover the load change. Also the PV unit does not participate in the power serving since it has reached its upper limit of current. Evidently, the smart participation of PHEVs has rescued the MG from an undesirable instable mode of operation.

#### 4.3.4. Power of PHEVs parking lot

The PHEVs active power in scenario 1 is depicted in Fig. 15, where the negative power means absorbing power from MG by PHEVs and vice the positive one means the injection to MG by PHEVs. looking at this figure, the non-smart charging based on previous participation strategy starts from  $t = 2$  s, by absorbing 60 kW active power. then at  $t = 3$  s, because of the load change in bus 9 the frequency falls instantly which causes the parking to decrease its charging power. Afterwards, the frequency is recovered and the parking continues drawing 60 kW active power by  $t = 8$  s. since the previous charging strategy had no sense of voltage, it doesn't response to voltage drops at all. At  $t = 8$  s, the PEMFC stops injecting power to the MG and because of the instability in the frequency; since the current-controlled inverter tends to rely on PLL to set the power set-point, the PHEVs parking lot can't continue its fixed charging and draws a random power from MG which cannot be relied on at all. The weakness of this strategy couldn't help the MG keep stable, but worsen its situation by random absorption of power.

The PHEVs active power in scenario 2 is demonstrated in Fig. 16 as the proposed smart charging scenario. as the proposed strategy reads both of voltage and frequency changes, it reacts to both of them. at  $t = 2$  s the PHEVs parking lot starts its smart-charging by drawing about 60 kW, it tracks the reference value by a small deviation. then at  $t = 3$  s,

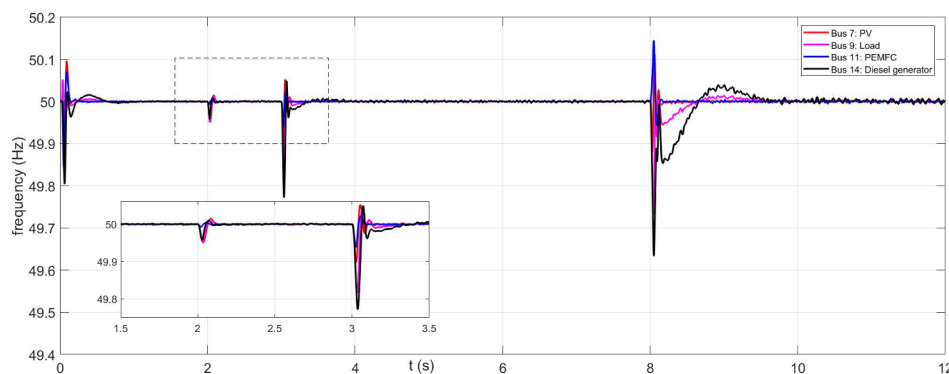


Fig. 10. MG frequency in scenario 2.

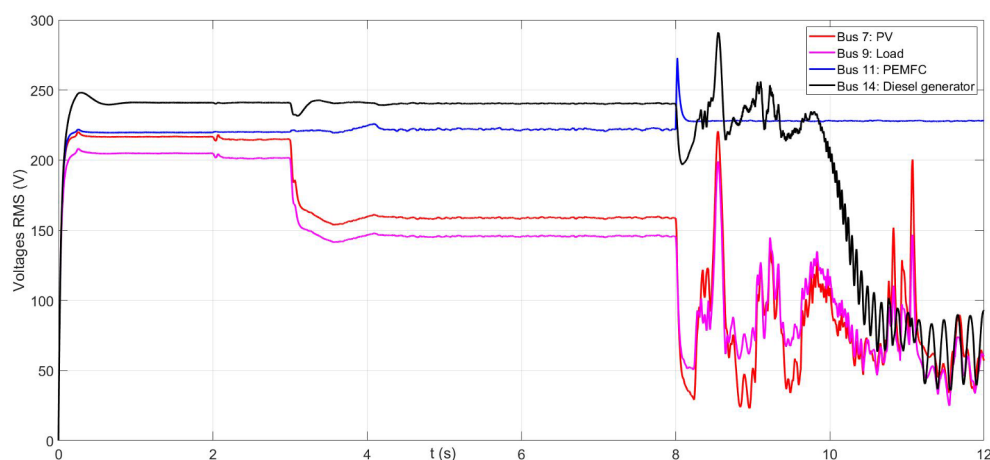


Fig. 11. MG voltages in scenario 1.

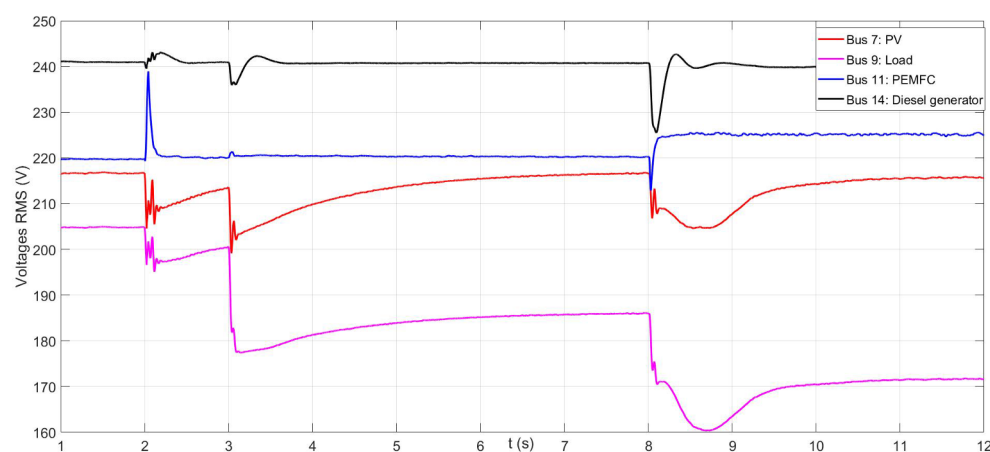


Fig. 12. MG voltages in scenario 2.

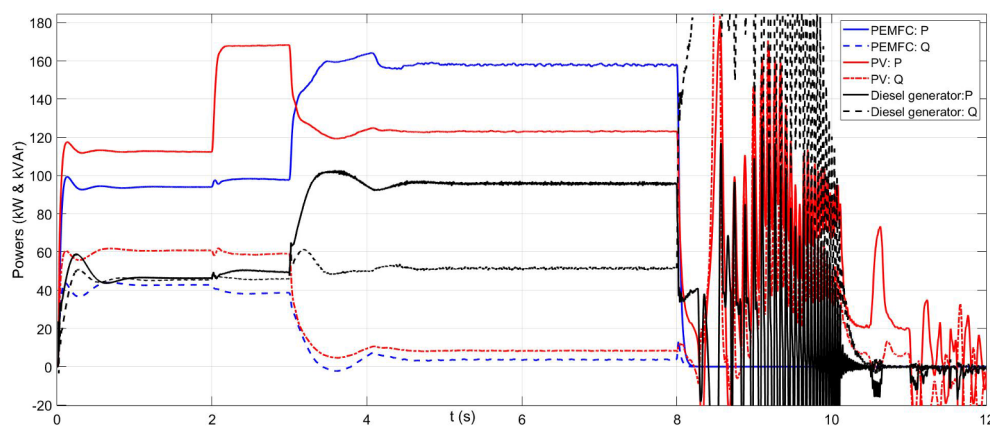


Fig. 13. DGs active and reactive powers in scenario 1.

the load change happens at bus 9 and the voltage falls at all buses, so the PHEVs parking lot lowers its charging power by  $t = 5$  s when the parking exchanges a small active power with the MG (8 kW). Afterwards, as a result of shutting down of PEMFC at  $t = 8$  s, the smart parking lot starts the injection of active power to the MG to mitigate the voltage and frequency deviations. as it is seen, the upper limit of parking lot limit its injection to the MG by 80 kW. as a result of the proposed strategy, the PHEVs can help to stabilize the MG in severe events.

## 5. Conclusions

Considering this fact that a line in a real MG has both resistance and reactance, an intelligent droop control is presented which is independent from the line parameters. This intelligent droop control is proposed to be implemented on all inverter-interfaced DGs except the PHEVs parking lot. Then a regular model is used for one or a bunch of PHEVs. As the main contribution, a novel strategy for participating the PHEVs in controlling the voltage and frequency of MGs is proposed and

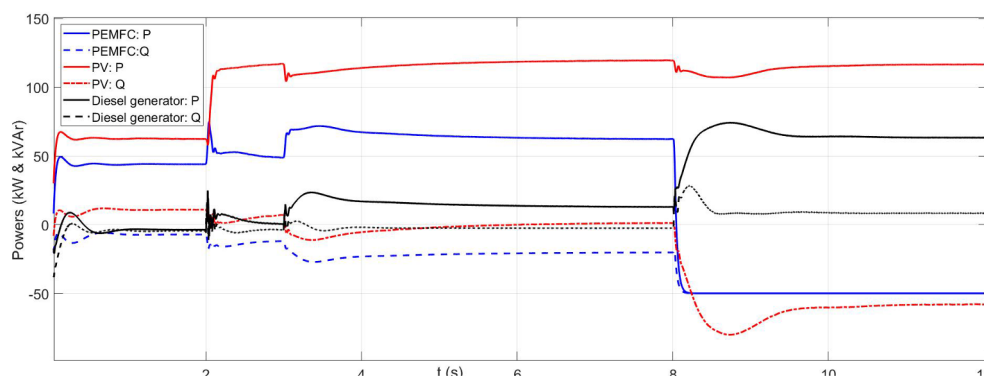


Fig. 14. DGs active and reactive powers in scenario 2.

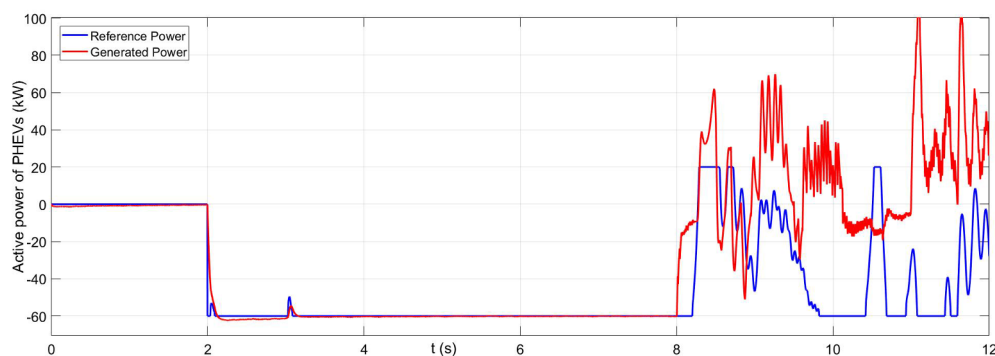


Fig. 15. PHEVs active power in scenario 1.

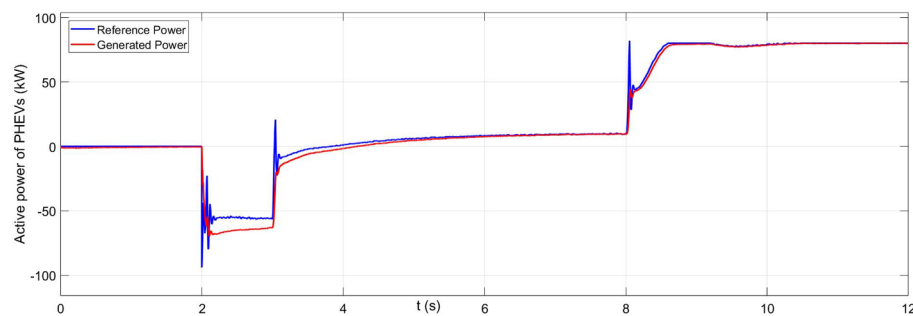


Fig. 16. PHEVs active power in scenario 2.

implemented which specifies the power command for the interface inverter considering both voltage and frequency of MG. The proposed strategy keeps the stability of the island MG better than another recent strategy. In the simulation studies, two modes of voltage and frequency control containing PHEVs in non-smart charging mode (scenario 1) and PHEVs smart charging mode (scenario 2) are implemented and compared. In non-smart charging scenario, the operation of PHEVs has aggravated the status of MG in the severe events and propels it towards instability; in contrast, the smart participation of PHEVs in the second scenario rescues the MG from instability, lowers the voltage drops and keeps the frequency constant during the events. It is verified that the individual PHEVs haven't been able to compensate all the voltage drops, so another technique of voltage restoration can perfect the operation of PHEVs and remove the voltage drops.

## 6. Future researches and recommendation

The prospective researches should focus on the modeling of PHEVs uncertainty and its effect on the voltage and frequency control of MGs which is essentially a dynamic power system problem. Some optimization techniques were reviewed in [25] which can be applied to perfect this study and even reach novel horizons. The authors are following this research work in Aalto university to implement it on cruise ships as a real island MG. Since the stability criteria of MGs are still under research, the MG stability is a major concern while growing the share of distributed converter-based DGs, so the future studies should possibly scrutinize the MGs stability in presence of a bunch of PHEVs dispersed in the MG.

## Appendix A

Full specifications of the implemented MG are presented in Tables 6 and 7 which is a modified form of the network introduced in [4]. Afterwards, the full specifications of the interfacing inverter are listed in Table 8.

**Table 6**  
Loads specifications for 14-bus test MG.

Load	Active power (kW)	Reactive power (kVAR)
LD8	19.125	11.835
LD9	70.11	43.47
LD10	59.94	37.125
LD12	92.025	56.88
LD13	19.125	11.835
Total	260.325	161.145

**Table 7**  
Lines specifications for 14-bus test MG.

Line	R ( $\Omega$ )	X ( $\Omega$ )	Line	R ( $\Omega$ )	X ( $\Omega$ )
L3	0.01988	0.00581	L9	0.00852	0.00249
L4	0.017395	0.00301	L10	0.02466	0.00231
L5	0.2583	0.00658	L11	0.38745	0.00987
L6	0.1449	0.00681	L12	0.0414	0.00246
L7	0.030485	0.002835	L13	0.0123	0.00231
L8	0.01491	0.00258	L14	0.00852	0.00249

**Table 8**  
Full Specifications of interfacing inverters (between DGs and MG).

Parameter	Value	Parameter	Value
$V_{L-L}$	380 V (rms)	$L_{Lc}$	0.1 mH
f	50 Hz	$r_{Lc}$	0.01 $\Omega$
$P_{nom}$	100 kW	$m_P$	$9.4 \times 10^{-5}$
$f_s$	6 kHz	$n_Q$	$1.3 \times 10^{-3}$
$L_f$	0.5 mH	R	0.05
$r_{Lf}, r_{Cf}$	0.01 $\Omega$	X	0.05
$C_f$	50 $\mu$ F	$\omega_C$	31.41
$V_{DC}$	500 V	F	0.75

## Appendix B. Supplementary material

Supplementary data associated with this article can be found, in the online version, at <https://doi.org/10.1016/j.ijepes.2019.03.036>.

## References

- [1] Gholami S, Aldeen M, Saha S. Control strategy for dispatchable distributed energy resources in Islanded microgrids. *IEEE Trans Power Syst* 2018;33(1):141–52.
- [2] Joung KW, Kim T, Park J. Decoupled frequency and voltage control for stand-alone microgrid with high renewable penetration. In: 2018 IEEE/IAS 54th industrial and commercial power systems technical conference (I&CPS), Niagara Falls, ON; 2018. p. 1–8.
- [3] Malik SM, Ai X, Sun Y, Zhengqi C, Shupeng Z. Voltage and frequency control strategies of hybrid AC/DC microgrid: a review. *IET Gen Transm Distrib* 2017;11(2):303–13.
- [4] Bevrani H, Shokoohi S. An intelligent droop control for simultaneous voltage and frequency regulation in Islanded microgrids. *IEEE Trans Smart Grid* 2013;4(3):1505–13.
- [5] Poornazaryan B, Abedi M, Gharehpetian GB, Shokoohi S. Suggested new voltage and frequency control framework for autonomous operation of microgrids. *AUT J Electric Eng* 2013;45(2):11–118.
- [6] John B, Ghosh A, Zare F. Load sharing in medium voltage Islanded microgrids with advanced angle droop control. *IEEE Trans Smart Grid* 2018;9(6):6461–9.
- [7] Dehkordi NM, Sadati N, Hamzeh M. Robust tuning of transient droop gains based on Kharitonov's stability theorem in droop-controlled microgrids. *IET Gen Transm Distrib* 2018;12(14):3495–501.
- [8] Raju P ESN, Jain Trapti. Robust optimal centralized controller to mitigate the small signal instability in an islanded inverter based microgrid with active and passive loads. *Int J Electric Power Energy Syst* 2017;90:225–36.
- [9] Mahmoud Magdi S, Alyazidi Nezar M, Abouheaf Mohamed I. Adaptive intelligent techniques for microgrid control systems: a survey. *Int J Electric Power Energy Syst* 2017;90:92–305.
- [10] Rokrok Ebrahim, Shafie-khah Miadreza, Catalão João PS. Review of primary voltage and frequency control methods for inverter-based islanded microgrids with distributed generation. *Renewable Sustain Energy Rev* 2018;82(3):3225–35.
- [11] Imran Rahman, Pandian Vasant, Balbir Singh, Abdullah-Al-Wadud M. Novel metaheuristic optimization strategies for plug-in hybrid electric vehicles: a holistic review. *Intell Decis Technol* 2016;10:149–63.
- [12] Imran Rahman, Junita Mohamad-Saleh. Plug-in electric vehicle charging optimization using bio-inspired computational intelligence methods. *Stud Syst Decis Control* 2018:135–47.

- [13] Farrokhbabadi M, Cañizares CA, Bhattacharya K. Frequency control in isolated/ Islanded microgrids through voltage regulation. *IEEE Trans Smart Grid* 2017;8(3):1185–94.
- [14] Serban I, Marinescu C. Control strategy of three-phase battery energy storage systems for frequency support in microgrids and with uninterrupted supply of local loads. *IEEE Trans Power Electron* 2014;29(9):5010–20.
- [15] Shotorbani, Mohammadpour Amin, Mohammadi-Ivatloo, Liwei Behnam Wang, Saeid Ghassem-Zadeh, Hossein Hosseini Seyed. Distributed secondary control of battery energy storage systems in a stand-alone microgrid. *IET Gen Transm Distrib* 2018;12(17):3944–53.
- [16] Sebastián R. Battery energy storage for increasing stability and reliability of an isolated Wind Diesel power system. *IET Renew Power Gen* 2017;11(2):296–303.
- [17] Urtasun A, Barrios EL, Sanchis P, Marroyo L. Frequency-based energy-management strategy for stand-alone systems with distributed battery storage. *IEEE Trans Power Electron* 2015;30(9):4794–808.
- [18] Morstyn T, Hredzak B, Agelidis VG. Distributed cooperative control of microgrid storage. *IEEE Trans Power Syst* 2015;30(5):2780–9.
- [19] Ersal T, Ahn C, Hiskens IA, Peng H, Stein JL. Impact of controlled plug-in EVs on microgrids: a military microgrid example. In: 2011 IEEE power and energy society general meeting, Detroit, MI, USA; 2011. p. 1–7.
- [20] Khooban Mohammad-Hassan, Niknam Taher, Blaabjerg Frede, Davari Pooya, Dragicevic Tomislav. A robust adaptive load frequency control for micro-grids. *ISA Trans* 2016;65:220–9.
- [21] Zhang Jing, Gao Yuan, Yu Peijia, Li Bowen, Yang Yan, Shi Ya, et al. Coordination control of multiple micro sources in islanded microgrid based on differential games theory. *Int J Electric Power Energy Syst* 2018;97:11–6.
- [22] Chen C, Duan S. Optimal integration of plug-in hybrid electric vehicles in micro-grids. *IEEE Trans Industr Inf* 2014;10(3):1917–26.
- [23] Pahasa J, Ngamroo I. PHEVs bidirectional charging/discharging and SoC control for microgrid frequency stabilization using multiple MPC. *IEEE Trans Smart Grid* 2015;6(2):526–33.
- [24] Almeida PMR, Lopes JAP, Soares FJ, Seca L. Electric vehicles participating in frequency control: operating islanded systems with large penetration of renewable power sources. In: 2011 IEEE Trondheim PowerTech, Trondheim; 2011. p. 1–6.
- [25] Rahman Imran, Vasant Pandian M, Singh Balbir, Singh Mahinder, Abdullah-Al-Wadud M, Adnan Nadia, et al. and electric vehicle charging infrastructures. *Renew Sustain Energy Rev* 2016;58:039–1047.
- [26] Rocha Almeida PM, Soares FJ, Peças Lopes JA. Electric vehicles contribution for frequency control with inertial emulation. *Electric Power Syst Res* 2015;127:141–50.
- [27] Prabha Kundur, Balu Neal J, Lauby Mark G. Power system stability and control. New York: McGraw-hill; 1994.
- [28] Hirase Yuko, Abe Kensho, Sugimoto Kazushige, Sakimoto Kenichi, Bevrani Hassan, Ise Toshifumi. A novel control approach for virtual synchronous generators to suppress frequency and voltage fluctuations in microgrids. *Appl Energy* 2018;210:699–710.
- [29] Pogaku N, Prodanovic M, Green TC. Modeling, analysis and testing of autonomous operation of an inverter-based microgrid. *IEEE Trans Power Electron* 2007;22(2):613–25.
- [30] Yazdani A, Iravani R. Voltage-sourced converters in power systems: modeling, control, and applications. John Wiley & Sons; 2010.
- [31] Meng Jian, Mu Yunfei, Jia Hongjie, Wu Jianzhong, Yu Xiaodan, Qu Bo. Dynamic frequency response from electric vehicles considering travelling behavior in the Great Britain power system. *Appl Energy* 2016;162:966–79.
- [32] Lee T, Hu S, Chan Y. Design of D-STATCOM for voltage regulation in Microgrids. In: 2010 IEEE energy conversion congress and exposition, Atlanta, GA; 2010. p. 3456–63.
- [33] Mohan N, Undeland TM. Power electronics: converters, applications, and design. India: Wiley; 2007.